INTERNATIONAL JOURNAL FOR NUMERICAL METHODS IN ENGINEERING
Int. J. Numer. Meth. Engng 2004; **60**:27–50 (DOI: 10.1002/nme.953)

Multiphase flow in deforming porous material

B. A. Schrefler*,†

Department of Structural and Transportation Engineering, Università degli Studi di Padova, via F. Marzolo 9, I-35131 Padova, Italy

SUMMARY

A model for mechanical behaviour of saturated–unsaturated porous media is presented within the framework of thermodynamics of irreversible processes. It includes interfaces with thermodynamic properties between the constituents. The necessary balance equations are derived using averaging theories. Restrictions on the form of the constitutive equations are obtained by exploiting the entropy inequality according to the Coleman–Noll procedure. A particular form of the governing equations is then solved numerically. The validation of the model proposed through a comparison between experimental and numerical results and an application example concerning a tunnel fire conclude the paper. Copyright © 2004 John Wiley & Sons, Ltd.

KEY WORDS: porous material; multiphase; effective stresses

1. INTRODUCTION

Multiphase porous media, i.e. porous media where the pores are filled by more than one fluid, are treated here within the framework of averaging theories. In particular, the approach developed by Hassanizadeh and Gray [1–4] is used.

The isothermal case was shown in Reference [5]. Here the approach is extended to non-isothermal situations. It is recalled that interfaces between the constituents with their thermodynamic properties are taken into account. In fact, fluids in a porous medium, such as gas and water, will remain immiscible only if there are interfaces with non-zero surface tension. If surface tension is zero, then capillary pressure is zero too which means that the fluid pressure will be equal all the time. Actually only averaging theories such as that used here include explicitly interfacial properties.

As far as the constitutive relationships are concerned, limits to their form are obtained by systematic exploitation of the entropy inequality, following the procedure of Coleman and Noll

*Correspondence to: B. A. Schrefler, Department of Structural and Transportation Engineering, Università degli Studi di Padova, via F. Marzolo 9, I-35131 Padova, Italy.
†E-mail: bas@caronte.dic.unipd.it

Contract/grant sponsor: EU Research fund MÆCENAS

Received 10 May 2003
Accepted 1 June 2003

[6]. Particular attention will be paid to near equilibrium results, which among others yield the well-known laws of Darcy, Fick and Fourier, augmented by the contributions of the interfaces.

From the general mathematical model a simplified one is extracted, which will be solved numerically. Particular attention is focused here on the boundary conditions: for a realistic simulation of heat and mass transfer problems in deforming porous media boundary conditions of the third type are needed which include convective mass transfer and convective and radiative heat transfer.

The theoretical developments in this paper are necessarily short. For a full development the reader is referred to the papers by Hassanizadeh and Gray [1–4], to Lewis and Schrefler [7] and to Schrefler [8]. An example dealing with behaviour of concrete structures during tunnel fires concludes the paper. The heat and mass transfer calculations in the tunnel needed as the input for the multiphase concrete model are also shown. The behaviour of concrete under such situations, where very high temperatures are reached, can be satisfactorily simulated only with an approach of the type presented here.

2. MACROSCOPIC BALANCE EQUATIONS

For sake of brevity the microscopic balance equations for the constituents of the porous medium are omitted here as well as the kinematics. They can be found e.g. in Reference [7]. In this section, the macroscopic balance equations for mass, linear momentum and energy as well as the entropy inequality are given, which have been obtained for the bulk material of the phases and for the interfaces by systematically applying the averaging procedures to the microscopic balance equations as outlined by Hassanizadeh and Gray [4]. The balance equations listed below have been specialized for a deforming porous material, where heat transfer and flow of water (liquid and vapour) and of dry air is taking place [7].

The constituents are assumed to be immiscible except for dry air and vapour, and chemically non-reacting. The mixture of dry air and vapour (moist air) will be simply called gas in the following. All fluids are in contact with the solid phase. Dissolution of air in water is here neglected. Stress is defined as tension positive for the solid phase, while pore pressure is defined as compressive positive for the fluids.

In the averaging procedure, volume density parameters η^π (volume fractions) appear which are expressed in terms of commonly used variables in multiphase flow: For solid phase, $\eta^\mathrm{s} = 1 - n$ where $n = (\mathrm{d}v^\mathrm{w} + \mathrm{d}v^\mathrm{g})/\mathrm{d}v$ is porosity and $\mathrm{d}v^\pi$ is the volume of constituent π within a representative elementary volume (REV); for water $\eta^\mathrm{w} = nS_\mathrm{w}$, where $S_\mathrm{w} = \mathrm{d}v^\mathrm{w}/(\mathrm{d}v^\mathrm{w} + \mathrm{d}v^\mathrm{g})$ is the degree of water saturation and for gas $\eta^\mathrm{g} = nS_\mathrm{g}$ with $S_\mathrm{g} = \mathrm{d}v^\mathrm{g}/(\mathrm{d}v^\mathrm{w} + \mathrm{d}v^\mathrm{g})$ the degree of gas saturation. It follows immediately that $S_\mathrm{w} + S_\mathrm{g} = 1$.

Also, there appear specific surfaces of the interfaces $a^{\alpha\beta}$, where the greek letters refer to the bulk phases involved. The inclusion of interface phenomena, which at first sight appear to be of secondary interest, allow to treat the dependence of phase properties on interface properties. At macroscale the system is modelled as the superposition of six continua: three phases and three interfaces. At every spatial point, average or macroscopic properties are defined for each continuum and the continua interact and exchange properties. Two sets of balance equations are needed. One set is for the bulk phases, the second is for the interfaces. The equations are listed next:

for solid

$$\frac{D^{\mathrm{s}}(1-n)\rho^{\mathrm{s}}}{Dt} + (1-n)\rho^{\mathrm{s}} \operatorname{div} \mathbf{v}^{\mathrm{s}} = \hat{e}^{\mathrm{s}}_{\mathrm{gs}} + \hat{e}^{\mathrm{s}}_{\mathrm{ws}} \tag{1}$$

for liquid water

$$\frac{D^{\mathrm{w}} n S_{\mathrm{w}} \rho^{\mathrm{w}}}{Dt} + n S_{\mathrm{w}} \rho^{\mathrm{w}} \operatorname{div} \mathbf{v}^{\mathrm{w}} = \hat{e}^{\mathrm{w}}_{\mathrm{gw}} + \hat{e}^{\mathrm{w}}_{\mathrm{sw}} \tag{2}$$

for gas

$$\frac{D^{\mathrm{g}} n S_{\mathrm{g}} \rho^{\mathrm{g}}}{Dt} + n S_{\mathrm{g}} \rho^{\mathrm{g}} \operatorname{div} \mathbf{v}^{\mathrm{g}} = \hat{e}^{\mathrm{g}}_{\mathrm{wg}} + \hat{e}^{\mathrm{g}}_{\mathrm{sg}} \tag{3}$$

where $\mathbf{v}^{\mathrm{s}}$, $\mathbf{v}^{\mathrm{w}}$, $\mathbf{v}^{\mathrm{g}}$ are the velocities of solid, liquid and gas phase, respectively. The mass source terms on the right-hand side (r.h.s) of Equations (1)–(3) correspond to exchange of mass with interfaces separating individual phases (phase changes) and couple these equations with the corresponding balance equations written for the interfaces. These last ones may be written as

$$\frac{D^{\alpha\beta} a^{\alpha\beta} \Gamma^{\alpha\beta}}{Dt} + a^{\alpha\beta} \Gamma^{\alpha\beta} \operatorname{div} \mathbf{w}^{\alpha\beta} = -\hat{e}^{\alpha}_{\alpha\beta} - \hat{e}^{\beta}_{\alpha\beta} + \hat{e}^{\alpha\beta}_{\mathrm{wgs}} \tag{4}$$

where $\mathbf{w}^{\alpha\beta}$ and $\Gamma^{\alpha\beta}$ are the mass weighted velocity and the density of the $\alpha\beta$ interface ($\alpha, \beta =$ s, w, g). The last term in Equations (4) describes mass exchange of the interfaces with their contact line. Since we have three phases composing the medium, there is only one contact line. This contact line does not have thermodynamic properties. The momentum balance equations for the bulk phases are:

for solid

$$(1-n)\rho^{\mathrm{s}} \frac{D^{\mathrm{s}}\mathbf{v}^{\mathrm{s}}}{Dt} - \operatorname{div}((1-n)\mathbf{t}^{\mathrm{s}}) - (1-n)\rho^{\mathrm{s}}\mathbf{g} = \hat{\mathbf{T}}^{\mathrm{s}}_{\mathrm{sg}} + \hat{\mathbf{T}}^{\mathrm{s}}_{\mathrm{sw}} \tag{5}$$

for water

$$nS^{\mathrm{w}}\rho^{\mathrm{w}} \frac{D^{\mathrm{w}}\mathbf{v}^{\mathrm{w}}}{Dt} - \operatorname{div}(nS_{\mathrm{w}}\mathbf{t}^{\mathrm{w}}) - (nS_{\mathrm{w}})\rho^{\mathrm{w}}\mathbf{g} = \hat{\mathbf{T}}^{\mathrm{w}}_{\mathrm{wg}} + \hat{\mathbf{T}}^{\mathrm{w}}_{\mathrm{ws}} \tag{6}$$

for gas

$$nS^{\mathrm{g}}\rho^{\mathrm{g}} \frac{D^{\mathrm{g}}\mathbf{v}^{\mathrm{g}}}{Dt} - \operatorname{div}(nS_{\mathrm{g}}\mathbf{t}^{\mathrm{g}}) - (nS_{\mathrm{g}})\rho^{\mathrm{g}}\mathbf{g} = \hat{\mathbf{T}}^{\mathrm{g}}_{\mathrm{gw}} + \hat{\mathbf{T}}^{\mathrm{g}}_{\mathrm{gs}} \tag{7}$$

where $\mathbf{t}^{\alpha}$ is the partial stress tensor, which is symmetric, $\mathbf{g}$ is the gravity vector and $\hat{\mathbf{T}}^{\alpha}_{\alpha\beta}$ describes the supply of momentum from the interfaces.

The r.h.s. terms in Equations (5)–(7) describe supply of momentum from the interfaces, i.e. related to phase changes. Analogous balance equations can be written for the momentum of the three interfaces:

$$\begin{aligned} a^{\alpha\beta}\Gamma^{\alpha\beta} \frac{D^{\alpha\beta}\mathbf{w}^{\alpha\beta}}{Dt} - \operatorname{div}\left(a^{\alpha\beta}\mathbf{s}^{\alpha\beta}\right) - a^{\alpha\beta}\Gamma^{\alpha\beta}\mathbf{g}^{\alpha\beta} \\ = -\left(\mathbf{T}^{\alpha}_{\alpha\beta} + \hat{e}^{\alpha}_{\alpha\beta}\mathbf{v}^{\alpha,\mathrm{s}}\right) - \left(\hat{\mathbf{T}}^{\beta}_{\alpha\beta} + \hat{e}^{\beta}_{\alpha\beta}\mathbf{v}^{\beta,\mathrm{s}}\right) + \left(\hat{e}^{\alpha}_{\alpha\beta} + \hat{e}^{\beta}_{\alpha\beta}\right)\mathbf{w}^{\alpha\beta,\mathrm{s}} + \hat{\mathbf{s}}^{\alpha\beta}_{\mathrm{wgs}} \end{aligned} \tag{8}$$

where $\mathbf{s}^{\alpha\beta}$ is the surface stress tensor, which is also symmetric.

The last r.h.s. term corresponds to momentum supply from the contact line wgs to the $\alpha\beta$ interface.

The energy balance equation for the bulk phases may be written as follows:

for solid

$$(1-n)\rho^{\mathrm{s}}\frac{D^{\mathrm{s}}E^{\mathrm{s}}}{Dt} - (1-n)\mathbf{t}^{\mathrm{s}} : \operatorname{grad}\mathbf{v}^{\mathrm{s}} - \operatorname{div}((1-n)\mathbf{q}^{\mathrm{s}}) - (1-n)\rho^{\mathrm{s}}h^{\mathrm{s}} = \hat{Q}^{\mathrm{s}}_{\mathrm{sw}} + \hat{Q}^{\mathrm{s}}_{\mathrm{sg}} \tag{9}$$

for water

$$nS_{\mathrm{w}}\rho^{\mathrm{w}}\frac{D^{\mathrm{w}}E^{\mathrm{w}}}{Dt} - nS_{\mathrm{w}}\mathbf{t}^{\mathrm{w}} : \operatorname{grad}\mathbf{v}^{\mathrm{w}} - \operatorname{div}(nS_{\mathrm{w}}\mathbf{q}^{\mathrm{w}}) - nS_{\mathrm{w}}\rho^{\mathrm{w}}h^{\mathrm{w}} = \hat{Q}^{\mathrm{w}}_{\mathrm{ws}} + \hat{Q}^{\mathrm{w}}_{\mathrm{wg}} \tag{10}$$

for gas

$$nS_{\mathrm{g}}\rho^{\mathrm{g}}\frac{D^{\mathrm{g}}E^{\mathrm{g}}}{Dt} - nS_{\mathrm{g}}\mathbf{t}^{\mathrm{g}} : \operatorname{grad}\mathbf{v}^{\mathrm{g}} - \operatorname{div}(nS_{\mathrm{g}}\mathbf{q}^{\mathrm{g}}) - nS_{\mathrm{g}}\rho^{\mathrm{g}}h^{\mathrm{g}} = \hat{Q}^{\mathrm{g}}_{\mathrm{gs}} + \hat{Q}^{\mathrm{g}}_{\mathrm{gw}} \tag{11}$$

The source terms in Equations (9)–(11) describe supply of heat to bulk phase from the interfaces, related to phase changes, while $\mathbf{q}^{\alpha}$ and h^{α} are the heat flux vector and the intrinsic heat source for the bulk phase α, respectively. The energy balance equations for the three interfaces read

$$\begin{aligned} a^{\alpha\beta}\Gamma^{\alpha\beta}\frac{D^{\alpha\beta}E^{\alpha\beta}}{Dt} - a^{\alpha\beta}\mathbf{s}^{\alpha\beta} : \operatorname{grad}\mathbf{w}^{\alpha\beta} - \operatorname{div}(a^{\alpha\beta}\mathbf{q}^{\alpha\beta}) - a^{\alpha\beta}\Gamma^{\alpha\beta}h^{\alpha\beta} \\ = -\left[\hat{Q}^{\alpha}_{\alpha\beta} + \hat{\mathbf{T}}^{\alpha}_{\alpha\beta}\cdot\mathbf{v}^{\alpha,\alpha\beta} + \hat{e}^{\alpha}_{\alpha\beta}(E^{\alpha,\alpha\beta} + \tfrac{1}{2}(v^{\alpha,\alpha\beta})^2)\right] \\ -\left[\hat{Q}^{\beta}_{\alpha\beta} + \hat{\mathbf{T}}^{\beta}_{\alpha\beta}\cdot\mathbf{v}^{\beta,\alpha\beta} + \hat{e}^{\beta}_{\alpha\beta}(E^{\beta,\alpha\beta} + \tfrac{1}{2}(v^{\beta,\alpha\beta})^2)\right] + \hat{Q}^{\alpha\beta}_{\mathrm{wgs}} \end{aligned} \tag{12}$$

where $E^{\alpha,\alpha\beta} = E^{\alpha} - E^{\alpha\beta}$.

The terms in square brackets in Equation (12) describe the energy supply from the bulk phase to the interface, energy associated with momentum supply and energy related to mass supply because of phase changes. The last r.h.s. term is supply of heat to the interface from the contact line.

We assume that entropy fluxes are due solely to heat input and the entropy external source terms are due only to external energy sources. Thus, the entropy balance may be expressed for the bulk phases as follows:

for solid

$$(1-n)\rho^{\mathrm{s}}\frac{D^{\mathrm{s}}\lambda^{\mathrm{s}}}{Dt} - \operatorname{div}\left((1-n)\frac{\mathbf{q}^{\mathrm{s}}}{\theta^{\mathrm{s}}}\right) - (1-n)\rho^{\mathrm{s}}\frac{h^{\mathrm{s}}}{\theta^{\mathrm{s}}} = \hat{\Phi}^{\mathrm{s}}_{\mathrm{sg}} + \hat{\Phi}^{\mathrm{s}}_{\mathrm{sw}} + \Lambda^{\mathrm{s}} \tag{13}$$

for water

$$nS_{\mathrm{w}}\rho^{\mathrm{w}}\frac{D^{\mathrm{w}}\lambda^{\mathrm{w}}}{Dt} - \operatorname{div}\left(nS_{\mathrm{w}}\frac{\mathbf{q}^{\mathrm{w}}}{\theta^{\mathrm{w}}}\right) - nS_{\mathrm{w}}\rho^{\mathrm{w}}\frac{h^{\mathrm{w}}}{\theta^{\mathrm{w}}} = \hat{\Phi}^{\mathrm{w}}_{\mathrm{wg}} + \hat{\Phi}^{\mathrm{w}}_{\mathrm{ws}} + \Lambda^{\mathrm{w}} \tag{14}$$

for gas

$$nS_{\mathrm{g}}\rho^{\mathrm{g}}\frac{D^{\mathrm{g}}\lambda^{\mathrm{g}}}{Dt}-\operatorname{div}\left(nS_{\mathrm{g}}\frac{\mathbf{q}^{\mathrm{g}}}{\theta^{\mathrm{g}}}\right)-nS_{\mathrm{g}}\rho^{\mathrm{g}}\frac{h^{\mathrm{g}}}{\theta^{\mathrm{g}}}=\hat{\Phi}^{\mathrm{g}}_{\mathrm{gw}}+\hat{\Phi}^{\mathrm{g}}_{\mathrm{gs}}+\Lambda^{\mathrm{g}} \tag{15}$$

where λ^{s}, λ^{w}, λ^{g}, are the entropy of the three phases and θ^{s}, θ^{w}, θ^{g}, are the absolute temperatures of the solid, liquid and gas phase, respectively. The two first terms in r.h.s. of Equations (13)–(15) describe the entropy supply to the bulk phases from the interfaces, while the last one is the rate of net production of entropy in the bulk phase.

Similarly, for the interfaces we have the following three entropy balance equations:

$$a^{\alpha\beta}\Gamma^{\alpha\beta}\frac{D^{\alpha\beta}\lambda^{\alpha\beta}}{Dt}-\operatorname{div}\left(a^{\alpha\beta}\frac{\mathbf{q}^{\alpha\beta}}{\theta^{\alpha\beta}}\right)-a^{\alpha\beta}\Gamma^{\alpha\beta}\frac{h^{\alpha\beta}}{\theta^{\alpha\beta}}=-\left(\hat{\Phi}^{\alpha}_{\alpha\beta}+\hat{e}^{\alpha}_{\alpha\beta}\lambda^{\alpha,\alpha\beta}\right)-\left(\hat{\Phi}^{\beta}_{\alpha\beta}+\hat{e}^{\beta}_{\alpha\beta}\lambda^{\beta,\alpha\beta}\right)+\hat{\Phi}^{\alpha\beta}_{\mathrm{wgs}}+\Lambda^{\alpha\beta} \tag{16}$$

The terms in parentheses in the r.h.s. of Equation (16) are supply of entropy from the interfaces and resulting from mass supply (phase change), the last but one accounts for entropy supply to the interface from the contact line and the last one is the rate of net production of entropy in the interface.

The terms related to exchange of mass, momentum, energy and entropy between interfaces via the contact lines must satisfy some restrictions, because the contact lines do not possess any thermodynamic properties as already stated. Thus, the following relations hold:

$$\begin{aligned}
\sum_{\alpha\beta}\hat{e}^{\alpha\beta}_{\mathrm{wgs}}&=0\\
\sum_{\alpha\beta}\left(\hat{\mathbf{s}}^{\alpha\beta}_{\mathrm{wgs}}+\hat{e}^{\alpha\beta}_{\mathrm{wgs}}\mathbf{w}^{\alpha\beta}\right)&=0\\
\sum_{\alpha\beta}\left[\hat{Q}^{\alpha\beta}_{\mathrm{wgs}}+\hat{\mathbf{s}}^{\alpha\beta}_{\mathrm{wgs}}\cdot\mathbf{w}^{\alpha\beta}+\hat{e}^{\alpha\beta}_{\mathrm{wgs}}\left(E^{\alpha\beta}+\tfrac{1}{2}\left(\mathbf{w}^{\alpha\beta}\right)^2\right)\right]&=0\\
\sum_{\alpha\beta}\left(\hat{\Phi}^{\alpha\beta}_{\mathrm{wgs}}+\hat{e}^{\alpha\beta}_{\mathrm{wgs}}\lambda^{\alpha\beta}\right)&=0
\end{aligned} \tag{17}$$

3. THE SECOND LAW OF THERMODYNAMICS

The balance laws must be supplemented with the second law of thermodynamics, which states that for any process the rate of net entropy production must be non-negative

$$\Lambda=\Lambda^{\mathrm{s}}+\Lambda^{\mathrm{w}}+\Lambda^{\mathrm{g}}+\sum_{\alpha\beta=\mathrm{gs,gw,sw}}\Lambda^{\alpha\beta}\geqslant 0 \tag{18}$$

where Λ^{π} is the rate of net production of entropy in the bulk phases and interfaces and $\alpha\beta=\mathrm{gs,gw,sw}$ refer to the interfaces between gas and solid, gas and water and water and solid, respectively.

After introducing the balance laws into Equation (18) and substituting the internal energy by the Helmholtz free energy, which is defined for the bulk phases as

$$A^{\alpha} = E^{\alpha} - \theta^{\alpha}\lambda^{\alpha}, \quad \alpha = \mathrm{s, w, g} \tag{19}$$

and for the interfaces as

$$A^{\alpha\beta} = E^{\alpha\beta} - \theta^{\alpha\beta}\lambda^{\alpha\beta}, \quad \alpha\beta = \mathrm{gw, ws, gs} \tag{20}$$

an appropriate form of the entropy inequality (18) is obtained [4]. The balance equations of mass, momentum and energy must be supplemented by constitutive equations describing the behaviour of individual phases. In total, there are 30 equations and the same number of independent variables can be chosen as basic independent fields. These field quantities or/and combinations and space and time derivatives of them that are objective can enter as independent constitutive variables. Their choice should be based on the expected behaviour of the medium, as well as they should account macroscopically for the microstructure due to the interfaces. For this last reason for instance volume fractions, their gradients, the specific surfaces of the interfaces and their gradients may be added to the list of primary variables. This augments accordingly the list of dependent variables to eliminate the ensuing equation deficit. The independent variables are function of time and space. The list of independent variables chosen here is ρ^{α}, $\Gamma^{\alpha\beta}$, $\mathbf{v}^{\alpha,\mathrm{s}}$, $\mathbf{w}^{\alpha\beta,\mathrm{s}}$, $\mathbf{E}^{\alpha}$, θ^{α}, $\operatorname{grad}\theta^{\alpha}$, $\theta^{\alpha\beta}$, $\operatorname{grad}\theta^{\alpha\beta}$, n, $\operatorname{grad} n$, S_{α}, $\operatorname{grad} S_{\alpha}$, $a^{\alpha\beta}$, $\operatorname{grad} a^{\alpha\beta}$.

The remaining variables appearing in the balance equations must be expressed in terms of the primary unknowns and their derivatives. The equation deficit is eliminated by also requiring constitutive forms for some of the time derivatives, (here of porosity, the degree of water saturation and of specific surfaces of the interfaces, [4]) and by thermodynamic equilibrium equations. For the list of dependent variables, for which constitutive relations are needed, see Reference [5].

Helmholtz free energy for the bulk phases is assumed to have the following functional form which is particularly simple, but sufficient for our purpose:

$$A^{\mathrm{w}} = A^{\mathrm{w}}(\rho^{\mathrm{w}}, \theta^{\mathrm{w}}, S_{\mathrm{w}}) \tag{21}$$

$$A^{\mathrm{g}} = A^{\mathrm{g}}(\rho^{\mathrm{g}}, \theta^{\mathrm{g}}, S_{\mathrm{g}}) \tag{22}$$

$$A^{\mathrm{s}} = A^{\mathrm{s}}(\rho^{\mathrm{s}}, \theta^{\mathrm{s}}, \mathbf{E}^{\mathrm{s}}, S_{\mathrm{w}}) \tag{23}$$

and for the interfaces

$$A^{\alpha\beta} = A^{\alpha\beta}(\Gamma^{\alpha\beta}, \theta^{\alpha\beta}, a^{\alpha\beta}, S_{\mathrm{w}}) \quad \text{where } \alpha\beta = \mathrm{gw, ws, gs} \tag{24}$$

All remaining dependent variables are allowed to depend on the complete set of independent variables given above. Note that assumptions (21)–(24) depart from the principle of equipresence.

According to the principle of admissibility, the constitutive postulates relating dependent to independent variables must not violate the balance laws and the entropy inequality. These requirements are satisfied using the procedure proposed by Coleman and Noll [6]. The rather lengthy transformations of the entropy inequality necessary are omitted here. They can be found in References [4, 8].

Following the procedure of Coleman–Noll the following non-equilibrium results are obtained:

$$\lambda^{\alpha} = -\frac{\partial A^{\alpha}}{\partial \theta^{\alpha}}, \quad \alpha = \mathrm{w}, \mathrm{g}, \mathrm{s} \tag{25}$$

$$\lambda^{\alpha\beta} = -\frac{\partial A^{\alpha\beta}}{\partial \theta^{\alpha\beta}}, \quad \alpha\beta = \mathrm{gw}, \mathrm{ws}, \mathrm{gs} \tag{26}$$

$$\mathbf{t}^{\mathrm{w}} = -p^{\mathrm{w}}\mathbf{I} \tag{27}$$

$$\mathbf{t}^{\mathrm{g}} = -p^{\mathrm{g}}\mathbf{I} \tag{28}$$

$$\mathbf{t}^{\mathrm{s}} = \mathbf{t}^{\mathrm{s}}_{\mathrm{e}} - p^{\mathrm{s}}\mathbf{I} \tag{29}$$

where

$$\mathbf{t}^{\mathrm{s}}_{\mathrm{e}} = \rho^{\mathrm{s}}(\mathbf{F}^{\mathrm{s}})^{\mathrm{T}} \cdot \frac{\partial A^{\mathrm{s}}}{\partial \mathbf{E}^{\mathrm{s}}} \cdot \mathbf{F}^{\mathrm{s}}$$

is the effective stress tensor of the solid phase ($\mathbf{F}^{\mathrm{s}}$ is the deformation gradient of the solid skeleton), and $p^{\mathrm{s}}(\rho^{\mathrm{s}}, \theta^{\mathrm{s}}, \mathbf{E}^{\mathrm{s}}, S^{\mathrm{w}}) = (\rho^{\mathrm{s}})^2\, \partial A^{\mathrm{s}}/\partial \rho^{\mathrm{s}}$ the thermodynamic pressure of the solid phase

$$\mathbf{s}^{\alpha\beta} = \gamma^{\alpha\beta}\mathbf{I} \tag{30}$$

where $\gamma^{\alpha\beta}$ is the surface tension.

3.1. Equilibrium restrictions

Some additional information can be obtained, when examining the system under consideration at equilibrium state where there is no relative movement of phases and interfaces, degree of saturation with water (thus also with gas) and porosity are constant, the phases and interfaces have the same uniform temperature. At these conditions, the total rate of entropy production Λ equals to zero, i.e. reaches its minimum value. Thus, the necessary and sufficient conditions for Λ to be at minimum at equilibrium are

$$\left[\frac{\partial \Lambda}{\partial z_k}\right]_{\mathrm{eq}} = 0, \quad k = 1, \ldots, 46 \tag{31}$$

and

$$\left\| \left[\frac{\partial^2 \Lambda}{\partial z_k \partial z_m}\right]_{\mathrm{eq}} \right\| \quad \text{be positive semi-definite,} \quad k, m = 1, \ldots, 46 \tag{32}$$

where z_k are the variables which are equal to zero at equilibrium. Application of restriction (31) to the entropy inequality allows to obtain the following relations valid at equilibrium:

$$(p^{\mathrm{s}})_{\mathrm{eq}} = S_{\mathrm{g}} p^{\mathrm{g}} + S_{\mathrm{w}} p^{\mathrm{w}} \tag{33}$$

$$p^{\mathrm{c}} = (p^{\mathrm{g}} - p^{\mathrm{w}})_{\mathrm{eq}} \tag{34}$$

$$(\hat{\mathbf{T}}^{\mathrm{w}})_{\mathrm{eq}} = (\hat{\mathbf{T}}^{\mathrm{w}}_{\mathrm{ws}} + \hat{\mathbf{T}}^{\mathrm{w}}_{\mathrm{wg}})_{\mathrm{eq}} = p^{\mathrm{w}} \operatorname{grad}(nS_{\mathrm{w}}) - nS_{\mathrm{w}}\rho^{\mathrm{w}} \frac{\partial A^{\mathrm{w}}}{\partial S_{\mathrm{w}}} \operatorname{grad} S_{\mathrm{w}} \tag{35}$$

$$(\hat{\mathbf{T}}^{\mathrm{g}})_{\mathrm{eq}} = (\hat{\mathbf{T}}^{\mathrm{g}}_{\mathrm{gs}} + \hat{\mathbf{T}}^{\mathrm{g}}_{\mathrm{gw}})_{\mathrm{eq}} = p^{\mathrm{g}} \operatorname{grad}(nS_{\mathrm{g}}) - nS_{\mathrm{g}}\rho^{\mathrm{g}} \frac{\partial A^{\mathrm{g}}}{\partial S_{\mathrm{g}}} \operatorname{grad} S_{\mathrm{g}} \tag{36}$$

$$(\hat{\mathbf{s}}^{\alpha\beta}_{\mathrm{sgw}} - \hat{\mathbf{T}}^{\alpha}_{\alpha\beta} - \hat{\mathbf{T}}^{\beta}_{\alpha\beta})_{\mathrm{eq}} = -\gamma^{\alpha\beta} \operatorname{grad} a^{\alpha\beta} - a^{\alpha\beta}\Gamma^{\alpha\beta} \frac{\partial A^{\alpha\beta}}{\partial S_{\mathrm{w}}} \operatorname{grad} S_{\mathrm{w}}, \quad \alpha\beta = \mathrm{gw, ws, gs} \tag{37}$$

$$(\mathbf{q}^{\mathrm{s}})_{\mathrm{eq}} = (\mathbf{q}^{\mathrm{w}})_{\mathrm{eq}} = (\mathbf{q}^{\mathrm{g}})_{\mathrm{eq}} = \mathbf{0} \tag{38}$$

$$(\mathbf{q}^{\mathrm{gw}})_{\mathrm{eq}} = (\mathbf{q}^{\mathrm{ws}})_{\mathrm{eq}} = (\mathbf{q}^{\mathrm{gs}})_{\mathrm{eq}} = \mathbf{0} \tag{39}$$

$$(\hat{Q}^{\mathrm{gw}}_{\mathrm{sgw}})_{\mathrm{eq}} = (\hat{Q}^{\mathrm{ws}}_{\mathrm{sgw}})_{\mathrm{eq}} = (\hat{Q}^{\mathrm{gs}}_{\mathrm{sgw}})_{\mathrm{eq}} = 0 \tag{40}$$

$$(\hat{Q}^{\mathrm{s}}_{\alpha\beta})_{\mathrm{eq}} = (\hat{Q}^{\mathrm{w}}_{\alpha\beta})_{\mathrm{eq}} = (\hat{Q}^{\mathrm{g}}_{\alpha\beta})_{\mathrm{eq}} = 0, \quad \alpha\beta = \mathrm{gw, ws, gs} \tag{41}$$

$$G^{\alpha\beta,\mathrm{s}} = \left(A^{\alpha\beta,\mathrm{s}} - \frac{\gamma^{\alpha\beta,\mathrm{s}}}{\Gamma^{\alpha\beta,\mathrm{s}}} \right)_{\mathrm{eq}} = 0, \quad \alpha\beta = \mathrm{gw, ws, gs} \tag{42}$$

$$G^{\alpha\beta,\alpha} = \left(A^{\alpha\beta,\alpha} - \frac{\gamma^{\alpha\beta,\alpha}}{\Gamma^{\alpha\beta,\alpha}} \right)_{\mathrm{eq}} = 0, \quad \alpha, \beta = \mathrm{w, g, s} \quad \alpha \neq \beta \tag{43}$$

From the above relations, particularly important for subsequent discussions are: Equation (33) describing solid pressure and Equation (34) defining capillary pressure at equilibrium. The definition of capillary pressure shows that p^{c} depends on independent variables as follows:

$$p^{\mathrm{c}} = p^{\mathrm{c}}(S_{\mathrm{w}}, n, a^{\mathrm{wg}}, a^{\mathrm{ws}}, \theta, \rho^{\mathrm{w}}, \rho^{\mathrm{g}}, \Gamma^{\mathrm{wg}}, \Gamma^{\mathrm{ws}}, \Gamma^{\mathrm{gs}}) \tag{44}$$

At equilibrium, p^{c} is given by Equation (34). The capillary pressure is commonly assumed to be a function of S_{w}, ρ^{w} and ρ^{g}, n and θ. Equation (44) shows that also interfacial areas and surface densities play a role. Cases where surface densities may change and affect capillary pressure are when surfactants are present and change the character of the interfaces.

Equations (38) and (39) indicate that at equilibrium there is no heat transfer within the phases and interfaces, what is true for a wide class of practical problems, where a state of 'local thermal equilibrium' or, more general, 'local thermodynamic equilibrium' is assumed. Finally, at equilibrium the Gibbs free energy per unit mass for each phase and interface will be equal.

For subsequent discussions, attention is restricted more to the mechanical aspect of the problem and less to its thermal aspect. It is assumed that temperature differences between phases at a macroscopic point are negligible also near equilibrium which is acceptable for a large class of problems. For these cases, a state of local thermal equilibrium prevails such that all phases and interfaces will have the same temperature θ at a point, although it may still vary in space.

If the system is considered 'near' equilibrium some additional simplifications may be obtained, as far as the constitutive functions are concerned. In such situations, a linear dependence of constitutive functions (describing thermodynamic flows) on primary variables (thermodynamic potentials) may be postulated. Some of these linear relations are widely used in practice, like for example Darcy's law or Fick's law for fluid flow and Fourier's law. This will be dealt with in the next section. The fact that the constitutive assumptions are to be linearized does not influence any conclusion that may be drawn concerning the equilibrium state of the system (i.e. only the dynamic state will be influenced, [9]).

3.2. Linear theory and state equations

Linearization is now exploited for the purpose of constructing a model useful for the solution of practical engineering problems. As said in the previous section, the temperatures of all phases and interfaces are equal. Further the dynamics of the system is considered near equilibrium such that linear dependence of the constitutive functions on independent variables which go to zero at equilibrium may be postulated. In particular, the equation of motion of the two fluid phases and the three interfaces has been obtained in this way by Hassanizadeh and Gray [4]. The linearization procedure, including the restrictions imposed by the second law of thermodynamics is rather lengthy and only the results are given here for the motion of the fluid phases.

The fluid motion is relative to $\mathbf{v}^{\mathrm{s}}$ with the solution of the solid phase equation considered as decoupled from the movement of other phases and interfaces. By neglecting the effects of the motion of interfaces on the motion of the phases, the momentum equation for the fluids becomes

$$\frac{1}{nS_\alpha}\mathbf{R}_\alpha^\alpha \cdot \mathbf{v}^{\alpha,\mathrm{s}} = (-\operatorname{grad} p^\alpha + \rho^\alpha \mathbf{g}) + \frac{\Omega^\alpha}{S_\alpha}\operatorname{grad} S_\alpha, \quad \alpha = \mathrm{w}, \mathrm{g} \tag{45}$$

where the wettability potential Ω^α is defined by $\Omega^\alpha/S_\alpha = \partial A^\alpha/\partial S_\alpha$ and $\mathbf{R}_\alpha^\alpha$ is a material coefficient or function of the independent variables.

Equation (45) reduces directly to Darcy's law for single-phase fluid flow or for multiphase flow if the restriction $n|\Omega^\alpha \operatorname{grad} S_\alpha| \ll |\mathbf{R}_\alpha^\alpha \cdot \mathbf{v}^{\alpha,\mathrm{s}}|$ holds. This is assumed for the model of Section 4, even if the significance of the last term of Equation (45) is not yet established and would require experimental study. It is here assumed that $\mathbf{R}_\alpha^\alpha$ is invertible and takes for single-phase flow the form

$$\mathbf{K}^\alpha = \eta^\alpha (\mathbf{R}_\alpha^\alpha)^{-1} = \frac{\mathbf{k}}{\mu^\alpha}(\rho^\alpha, \eta^\alpha, T) \tag{46}$$

where μ^α is the dynamic viscosity, $\mathbf{k}$ the intrinsic permeability. T is the deviation of temperature θ from a reference value T_0 such that $T = \theta - T_0$. In case of more fluids flowing, the intrinsic permeability is modified as

$$\mathbf{k}^\alpha = k^{r\alpha}\mathbf{k} \tag{47}$$

with $k^{r\alpha}$ the relative permeability varying between 0 and 1, see Reference [10].

On similar lines Bennethum and Cushman, [11, 12] and Bennethum *et al.* [13] have derived Fick's law. Under assumption that the Helmholtz free energy of the bulk fluid phase α (and hence the chemical potential $\mu^{\alpha j}$) is a function of concentration within α, volume fractions,

interfacial area densities and density of bulk phase α Fick's law becomes [14]

$$R^{\alpha j}\mathbf{u}^{\alpha j} = -\eta^{\alpha}\rho^{\alpha j}\,\mathrm{grad}\,\mu^{\alpha j} = -\eta^{\alpha}\rho^{\alpha j}K^{\alpha 1}\,\mathrm{grad}\,C^{\alpha j} - \eta^{\alpha}\rho^{\alpha j}(K^{\alpha 2}\,\mathrm{grad}\,\eta^{\alpha} + K^{\alpha 3}\,\mathrm{grad}\,\eta^{\beta} + K^{\alpha 4}\,\mathrm{grad}\,a^{\alpha\beta} + K^{\alpha 5}\,\mathrm{grad}\,a^{\alpha s} + K^{\alpha 6}\,\mathrm{grad}\,\rho^{\alpha}) \tag{48}$$

where $\mathbf{u}^{\alpha j}$ is the diffusive velocity for constituent j in the bulk phase α, $R^{\alpha j}$ the linearization coefficient and $C^{\alpha j}$ the concentration of j in α. The coefficients K^{α^*} (*, 1–6) represent the change in chemical potential with respect to the appropriate independent variables e.g. $K^{\alpha 1}$is the change in chemical potential of αj with respect to $C^{\alpha j}$; the meaning of $K^{\alpha 2}$, $K^{\alpha 3}$, $K^{\alpha 6}$ is clear, from Equation (48) while $K^{\alpha 4}$ takes into account the amount of surface area between the two fluids $\alpha\beta$, which may or may not have a significant effect on diffusion within bulk phase α. $K^{\alpha 5}$ involves the solid interface. $K^{\alpha 2}$ and $K^{\alpha 3}$ are significant only if swelling is going on as in clay. The importance of $K^{\alpha 4}$, $K^{\alpha 5}$ and $K^{\alpha 6}$ has to be determined experimentally.

A similar equation can be written for the interface.

By assuming $A^{\alpha} = A^{\alpha}(\rho^{\alpha}, C^{\alpha j}, \theta)$, isothermal conditions and introducing an appropriate constitutive assumption for the linearization coefficient, Fick's law for a binary gas may be obtained as (see Reference [15])

$$\mathbf{J}_{\alpha}^{j} = -\eta^{\alpha}\mathbf{D}_{\alpha}^{j}\,\mathrm{grad}\left(\frac{\rho^{j}}{\rho^{\alpha}}\right) \tag{49}$$

where the diffusive dispersive mass flux $\mathbf{J}_{\alpha}^{j} = \eta^{\alpha}\rho^{\alpha}C^{\alpha j}\mathbf{u}^{\alpha j}$ of component j in phase α has been used, as in Equation (25), $\mathbf{D}_{\alpha}^{j}$ is the effective dispersion tensor given by $-\eta^{\alpha}\rho^{\alpha j}\mathbf{K}^{\alpha 1}/R^{\alpha j}$, j is the diffusing phase ($j = \mathrm{ga}, \mathrm{gw}$, ga and gw stand for dry air and water vapour respectively) and α the phase in which diffusion takes place ($\alpha = \mathrm{w}, \mathrm{g}$). For dry air and water vapour in particular $\mathbf{D}_{\mathrm{g}}^{\mathrm{ga}} = \mathbf{D}_{\mathrm{g}}^{\mathrm{gw}} = \mathbf{D}_{\mathrm{g}}$. This form of Fick's law will be used in the model of Section 4.

Also Fourier's law can be obtained by linearization in the form [4]

$$\sum_{\alpha}\eta^{\alpha}\mathbf{q}^{\alpha} + \sum_{\alpha\beta}a^{\alpha\beta}\mathbf{q}^{\alpha\beta} = \mathbf{K}\,\mathrm{grad}\,\theta \tag{50}$$

where $\mathbf{K}$ is again a material property. This equation, by neglecting the contribution of the interfaces, is used in the model of Section 4. Other results of linearization, which however do not enter into the model of Section 4, can be found in Reference [5].

As pointed out in the introduction, for the model closure state equations are still needed. Moist air (gas) in the pore system is assumed to be a perfect mixture of two ideal gases, dry air and water vapour. The equation of perfect gas is hence valid

$$p^{\mathrm{ga}} = \rho^{\mathrm{ga}}\theta R/M_{\mathrm{a}}, \quad p^{\mathrm{gw}} = \rho^{\mathrm{gw}}\theta R/M_{\mathrm{w}} \tag{51}$$

$$\rho^{\mathrm{g}} = \rho^{\mathrm{ga}} + \rho^{\mathrm{gw}}, \quad p^{\mathrm{g}} = p^{\mathrm{ga}} + p^{\mathrm{gw}}, \quad M_{\mathrm{g}} = \left(\frac{\rho^{\mathrm{gw}}}{\rho^{\mathrm{g}}}\frac{1}{M_{\mathrm{w}}} + \frac{\rho^{\mathrm{ga}}}{\rho^{\mathrm{g}}}\frac{1}{M_{\mathrm{a}}}\right)^{-1} \tag{52}$$

where R is the universal gas constant and M_{α} the molar mass of the constituents.

The equation of state of water is of the form $p^{\mathrm{w}} = p^{\mathrm{w}}(\rho^{\mathrm{w}}, T, S^{\mathrm{w}})$ [10].

4. HEAT AND MASS TRANSFER IN DEFORMING PARTIALLY SATURATED GEOMATERIALS

From the equations listed in the previous sections a model for heat and mass transfer in partially saturated geomaterials will now be established. The system of governing equations of this model will then be solved numerically. It is assumed that the system is near equilibrium as explained in the previous sections. Compared to the general theory outlined in the previous sections the model is simple, for instance, it does not consider the balance equations for the interfaces. However, compared to the models currently in use in the geomechanics community, it is rather advanced. It may be considered as a first step in the effort to obtain such thermodynamically based numerical models. Its complexity can then be augmented at will following the equations given in the theoretical section.

4.1. Simplified field equations

The model is built in the following way. From the linearized equations of Section 3.2 Fick's law is chosen in the form of Equation (49) and Fourier's law in the form of Equation (50), but neglecting interfacial terms. Instead of using Darcy's equation in the form of Equation (45), the linear momentum balance equation for the fluid phases is used directly with an appropriate constitutive assumption for the momentum exchange term in the form

$$\eta^\alpha \rho^\alpha \hat{\mathbf{t}}^\alpha = -\mathbf{R}^\alpha \eta^\alpha \mathbf{v}^{s\alpha} + p^\alpha \operatorname{grad} \eta^\alpha \tag{53}$$

where $\mathbf{R}^\alpha$ is given by Equation (46). This allows to consider indirectly the term $p^\alpha \operatorname{grad} \eta^\alpha$. These equations are supplemented by the mass balance equations for solid (1), water (2), vapour and gas (3), the sum of the linear momentum balance equation for constituents (5)–(7), and the sum of the energy balance equation for constituents (9)–(11), which has been transformed into an enthalpy balance (see Reference [7]). Further, for the fluid stresses, the solid pressure and the capillary pressure the respective equilibrium values are taken, Equations (27), (28), (33) and (34). The effective stress principle is assumed in the form

$$\mathbf{t} = (1 - n)\mathbf{t}_{\mathrm{e}}^{\mathrm{s}} - \mathbf{I}(S_{\mathrm{g}} p^{\mathrm{g}} + S_{\mathrm{w}} p^{\mathrm{w}}) \tag{54}$$

Finally, the state equations for water and gas Equations (51), (52) of Section 3.2 are used and the capillary pressure saturation relationship Equation (44) (with a much simpler functional dependence suggested by experimental observations $p^{\mathrm{c}} = p^{\mathrm{c}}(S_{\mathrm{w}}, \theta)$). Actually, the inverse of this function is used because of the choice of the primary variables.

This choice of primary variables needs some comments. Following experimental knowledge about the hydro-thermo-mechanical phenomena in porous media, displacements, temperatures, gas pressure and capillary pressure have been chosen here as primary variables. All other variables depend on these independent variables. Pressures have been chosen instead of the saturations because at the separation surface between two different porous media saturations usually experience a jump requiring the appropriate jump conditions while capillary pressures are continuous. Then capillary pressure has been chosen in preference to vapour pressure, because for fully saturated porous media vapour pressure has no physical meaning and close to fully saturated zones as e.g. in heated concrete, use of vapour pressure results in serious numerical problems. Capillary pressure can be used formally as variable also outside the capillary range as indicated below. This avoids changing model in the low moisture range when capillary water

is not present in the pores and capillary pressure has no physical meaning (see Reference [7]). Vapour pressure has to be expressed as function of the relevant primary variables capillary pressure and temperature. This is obtained by means of the Kelvin–Laplace equation, which is a thermodynamic relation at equilibrium (see References [16, 17]).

$$\frac{p^{\mathrm{gw}}}{p^{\mathrm{gws}}} = \exp\left(\frac{p^{\mathrm{c}} M_{\mathrm{w}}}{\rho^{\mathrm{w}} R\theta}\right) \tag{55}$$

where the vapour saturation pressure p^{gws} is obtained from the Clausius–Clapeyron equation.

Since the capillary pressure p^{c} is equal to the water potential Ψ^{w} multiplied by a constant ($p^{\mathrm{c}} = -\rho^{\mathrm{w}}\Psi^{\mathrm{w}}$), Equation (55) can also be used outside the capillary region [16, 17].

Some rearrangements of these equations (see Reference [7]) yield the following field equations. The macroscopic mass balance equations are: for the solid phase

$$\frac{1-n}{\rho^{\mathrm{s}}}\frac{D^{\mathrm{s}}\rho^{\mathrm{s}}}{Dt} - \frac{D^{\mathrm{s}}n}{Dt} + (1-n)\operatorname{div}\mathbf{v}^{\mathrm{s}} = 0 \tag{56}$$

for dry air

$$\begin{aligned} &-n\frac{D^{\mathrm{s}}S_{\mathrm{w}}}{Dt} - \beta_{\mathrm{s}}(1-n)S_{\mathrm{g}}\frac{D^{\mathrm{s}}T}{Dt} + S_{\mathrm{g}}\operatorname{div}\mathbf{v}^{\mathrm{s}} + \frac{S_{\mathrm{g}}n}{\rho^{\mathrm{ga}}}\frac{D^{\mathrm{s}}}{Dt}\left(\frac{M_{\mathrm{a}}}{\theta R}p^{\mathrm{ga}}\right) \\ &\quad - \frac{1}{\rho^{\mathrm{ga}}}\operatorname{div}\left[\rho^{\mathrm{g}}\frac{M_{\mathrm{a}}M_{\mathrm{w}}}{M_{\mathrm{g}}^2}\mathbf{D}_{\mathrm{g}}\operatorname{grad}\left(\frac{p^{\mathrm{ga}}}{p^{\mathrm{g}}}\right)\right] + \frac{1}{\rho^{\mathrm{ga}}}\operatorname{div}(nS_{\mathrm{g}}\rho^{\mathrm{ga}}\mathbf{v}^{\mathrm{gs}}) = 0 \end{aligned} \tag{57}$$

for the water species, i.e. liquid water and vapour together

$$\begin{aligned} &n(\rho^{\mathrm{w}}-\rho^{\mathrm{gw}})\frac{D^{\mathrm{s}}S_{\mathrm{w}}}{Dt} - \beta_{\mathrm{swg}}\frac{D^{\mathrm{s}}T}{Dt} + (\rho^{\mathrm{gw}}S_{\mathrm{g}}+\rho^{\mathrm{w}}S_{\mathrm{w}})\operatorname{div}\mathbf{v}^{\mathrm{s}} + \frac{n\,\rho^{\mathrm{w}}S_{\mathrm{w}}}{K_{\mathrm{w}}}\frac{D^{\mathrm{s}}p^{\mathrm{w}}}{Dt} + S_{\mathrm{g}}n\frac{D^{\mathrm{s}}}{Dt}\left(\frac{M_{\mathrm{w}}}{\theta R}p^{\mathrm{gw}}\right) \\ &\quad - \operatorname{div}\left[\rho^{\mathrm{g}}\frac{M_{\mathrm{a}}M_{\mathrm{w}}}{M_{\mathrm{g}}^2}\mathbf{D}_{\mathrm{g}}\operatorname{grad}\left(\frac{p^{\mathrm{gw}}}{p^{\mathrm{g}}}\right)\right] + \operatorname{div}\left\{\rho^{\mathrm{gw}}\frac{\mathbf{k}k^{\mathrm{rg}}}{\mu^{\mathrm{g}}}[-\operatorname{grad}p^{\mathrm{g}} + \rho^{\mathrm{g}}(\mathbf{g}-\mathbf{a}^{\mathrm{s}}-\mathbf{a}^{\mathrm{gs}})]\right\} \\ &\quad + \operatorname{div}\left\{\rho^{\mathrm{w}}\frac{\mathbf{k}k^{\mathrm{rw}}}{\mu^{\mathrm{w}}}[-\operatorname{grad}p^{\mathrm{w}} + \rho^{\mathrm{w}}(\mathbf{g}-\mathbf{a}^{\mathrm{s}}-\mathbf{a}^{\mathrm{ws}})]\right\} = 0 \end{aligned} \tag{58}$$

where

$$\beta_{\mathrm{swg}} = \beta_{\mathrm{s}}(1-n)(S_{\mathrm{g}}\rho^{\mathrm{gw}} + \rho^{\mathrm{w}}S_{\mathrm{w}}) + n\beta_{\mathrm{w}}\rho^{\mathrm{w}}S_{\mathrm{w}} \tag{59}$$

with β_π the thermal expansion coefficients.

The linear momentum balance equation for fluids is

$$\eta^{\pi}\mathbf{v}^{\pi\mathrm{s}} = \frac{\mathbf{k}k^{\mathrm{r}\pi}}{\mu}[-\operatorname{grad}p^{\pi} + \rho^{\pi}(\mathbf{g}-\mathbf{a}^{\mathrm{s}}-\mathbf{a}^{\pi\mathrm{s}})] \tag{60}$$

and for the multiphase medium

$$-\rho\mathbf{a}^{\mathrm{s}} - nS_{\mathrm{w}}\rho^{\mathrm{w}}[\mathbf{a}^{\mathrm{ws}} + \mathbf{v}^{\mathrm{ws}}\cdot\operatorname{grad}\mathbf{v}^{\mathrm{w}}] - nS_{\mathrm{g}}\rho^{\mathrm{g}}[\mathbf{a}^{\mathrm{gs}} + \mathbf{v}^{\mathrm{gs}}\cdot\operatorname{grad}\mathbf{v}^{\mathrm{g}}] + \operatorname{div}\mathbf{t} + \rho\mathbf{g} = 0 \tag{61}$$

Finally, the enthalpy balance for the multiphase medium may be written as

$$(\rho C_p)_{\text{eff}} \frac{\partial T}{\partial t} + (\rho_{\text{w}} C_{\text{p}}^{\text{w}} \mathbf{v}^{\text{w}} + \rho_{\text{g}} C_p^{\text{g}} \mathbf{v}^{\text{g}}) \cdot \text{grad}\, T - \text{div}(\chi_{\text{eff}} \text{grad}\, T) = -\dot{m} \Delta H_{\text{vap}} \tag{62}$$

where

$$(\rho C_p)_{\text{eff}} = \rho_{\text{s}} C_p^{\text{s}} + \rho_{\text{w}} C_p^{\text{w}} + \rho_{\text{g}} C_p^{\text{g}}, \quad \chi_{\text{eff}} = \chi^{\text{s}} + \chi^{\text{w}} + \chi^{\text{g}}, \quad \Delta H_{\text{vap}} = H^{\text{gw}} - H^{\text{w}} \tag{63}$$

with H^{π} the specific enthalpy and C_P^{π} the heat capacity.

4.2. Initial and boundary conditions

The initial conditions specify the full fields of gas pressure, capillary or water pressure, temperature, displacements and velocities

$$\begin{aligned} p^{\text{g}} &= p_0^{\text{g}}, \quad p^{\text{c}} = p_0^{\text{c}}, \quad T = T_0 \\ \mathbf{u} &= \mathbf{u}_0, \quad \dot{\mathbf{u}} = \dot{\mathbf{u}}_0, \quad \text{at } t = t_0 \end{aligned} \tag{64}$$

The boundary conditions are formulated for volume-averaged quantities, which are continuous fields. Thus, they concern an arbitrary boundary of the analysed space domain which corresponds to the 'macroscopic' external surface of the porous body coinciding with its fixed boundary considered during volume averaging.

The boundary conditions can be imposed values on Γ_π or fluxes on Γ_π^q, where the boundary $\Gamma = \Gamma_\pi \cup \Gamma_\pi^q$. The imposed values on the boundary for gas pressure, capillary or water pressure, temperature and displacements are

$$\begin{aligned} p^{\text{g}} &= \hat{p}^{\text{g}} \text{ on } \Gamma_{\text{g}}, \quad p^{\text{c}} = \hat{p}^{\text{c}} \text{ on } \Gamma_{\text{c}} \\ T &= \hat{\mathbf{T}} \text{ on } \Gamma_T, \quad \mathbf{u} = \hat{\mathbf{u}} \text{ on } \Gamma_u \end{aligned} \tag{65}$$

The volume-averaged flux boundary conditions for water species and dry air mass balance equations and the energy conservation equation, to be imposed at the interface between the porous media and the surrounding fluid are as follows:

$$\begin{aligned} (\rho^{\text{ga}} \bar{\mathbf{v}}^{\text{g}} - \rho^{\text{g}} \bar{\mathbf{v}}^{\text{gw}}) \cdot \mathbf{n} &= q^{\text{ga}} \quad \text{on } \Gamma_{\text{g}}^q \\ (\rho^{\text{gw}} \bar{\mathbf{v}}^{\text{g}} + \rho^{\text{w}} \bar{\mathbf{v}}^{\text{w}} + \rho^{\text{g}} \bar{\mathbf{v}}^{\text{gw}}) \cdot \mathbf{n} &= \beta_{\text{c}} (\rho^{\text{gw}} - \rho_\infty^{\text{gw}}) + q^{\text{gw}} + q^{\text{w}} \quad \text{on } \Gamma_{\text{c}}^q \\ -(\rho^{\text{w}} \bar{\mathbf{v}}^{\text{w}} \Delta h_{\text{vap}} - \chi_{\text{eff}} \nabla T) \cdot \mathbf{n} &= \alpha_{\text{c}} (T - T_\infty) + \sigma_0 \varepsilon (T^4 - T_\infty^4) + q^T \quad \text{on } \Gamma_T^q \end{aligned} \tag{66}$$

where $\mathbf{n}$ is the unit vector, perpendicular to the surface of the porous medium, pointing toward the surrounding gas, ρ_∞^{gw} and T_∞ are, respectively, the mass concentration of water vapour and temperature in the undisturbed gas phase distant from the interface, α_{c}, β_{c}, σ_0 and ε are convective heat and mass transfer coefficients, the Boltzmann constant and the emissivity, while $q^{\text{ga}}, q^{\text{gw}}, q^{\text{w}}$ and q^{T} are the imposed dry air flux, imposed vapour flux, imposed liquid flux and imposed heat flux, respectively. The convective term on the r.h.s. of the last of Equations (66) corresponds to Newton's law of cooling and describes the conditions occurring in most practical situations at the interface between a porous medium and the surrounding fluid (air in this case). The traction boundary conditions for the displacement field are

$$\mathbf{t} \cdot \mathbf{n} = \hat{\hat{\mathbf{t}}} \quad \text{on } \Gamma_u^q \tag{67}$$

where $\hat{\hat{\mathbf{t}}}$ is the imposed traction.

5. BEHAVIOUR OF CONCRETE IN TUNNEL FIRES

We extend here the procedure outlined in Sections 2–4 to deal with the behaviour of concrete walls and ceilings in case of tunnel fires. The recent fires which occurred in major European tunnels (Channel, [18, 19], Mont-Blanc, Great Belt Link, Tauern, St Gotthard, etc.) emphasize the serious hazards they represent and the impact they may have on human beings, economy and repair costs. Extensive and heavy damage in the concrete elements were observed. The structural damage can be attributed to two main factors, namely, spalling of concrete and excessive temperatures attained in both concrete and steel components leading to serious loss of load bearing capacity. The temperature field inside the wall depends on the incident heat fluxes (convective and radiative), related to location and type of fire, air-flow rate through the tunnel and smoke properties.

The numerical simulation of such complex situations requires advanced numerical models which allow to simulate the fire scenario in the tunnel and the real physical behaviour of the concrete structure in such severe conditions. The behaviour of concrete can be satisfactorily simulated only with a multiphase porous media approach such as that used in this paper. In case of high temperatures, the following mass transport mechanisms take place in concrete: for capillary water we have Darcian-type flow and the thermodynamic force is the water pressure gradient; for adsorbed water there is diffusional flow and the force is the water concentration gradient. For chemically adsorbed water there is no transport, but it acts as source or sink term. Water vapour presents both Darcian flow under gas pressure gradient and diffusional flow under water vapour concentration gradient. Similarly dry air presents Darcian flow, also under gas pressure gradient and diffusional flow under dry air concentration gradient. All these phenomena can be modelled by the equations shown in Sections 3 and 4. Further, there are phase changes of chemical and physical nature: dehydration, evaporation and desorption which are endothermic processes, while hydration, condensation and adsorption are exothermic ones. All these require appropriate exchange terms in the balance equations, which have been introduced in References [17, 20–22]. As far as the fire scenario is concerned, this represents a boundary condition for the concrete wall and will be dealt with next.

5.1. Detailed thermal analysis

Prediction of the thermal field within a tunnel in presence of fire is quite complex, since combustion gives way to a combination of heat transfer phenomena (by convection, radiation and conduction) with strong interactions among them. As well known, in the reaction zone chemical energy is converted into internal energy of the products thus leading to convective movements of the fluid, as well as short wave radiation; at the same time mutual radiation takes place among the walls and to the other parts of the fluid, according to their temperatures and radiative properties.

A possible approach for the computer simulation of such complex phenomena will be discussed hereafter: firstly the sub-models of combustion, thermo-fluid dynamics, radiative heat transfer and thermal conduction will be separately described and then suitably linked together in order to account for their mutual influences.

5.1.1. Combustion. The 'Volumetric heat source (VHS)' [23] method assumes a given spatial and temporal distribution of the equivalent heat generation H per unit volume:

$$H = f(\mathbf{r}, t) \tag{68}$$

where $\mathbf{r}$ is the co-ordinate vector, and t the time. Usually, H is assumed to be constant throughout a given volume V representing the zone of reaction and therefore, being $Q(t)$ the overall heat generation:

$$H = Q(t)/V \tag{69}$$

Despite of its simplicity, this model appears to be reliable enough for enclosure fires, as shown by the experimental validations reported in Reference [23], and can therefore be applied with satisfactory confidence.

5.1.2. Thermo-fluid dynamics. The evaluation of air temperatures and velocities inside the tunnel, as well as convective heat transfer at its walls can be obtained by resorting to computational fluid dynamics (CFD). The energy balance equation is affected by the net equivalent heat generation/sink, due to the overall effect of chemical reactions and thermal radiation (absorbed and released by the fluid). The temperatures of the surrounding walls, as well as the heat generation/sink inside the fluid, represent boundary conditions which must be known beforehand.

5.1.3. Thermal radiation. Thermal radiation inside a tunnel with fire is quite complex since participating media (including smoke, soot, liquid droplets, ash and dust particles) are usually present in a wide range of temperatures and compositions. The 'Monte Carlo' statistical method is used to obtain the radiative heat flux of Equation (66) [24]. In principle, a point in the domain of the function is selected at random and, sampling from the probability distributions that model the physical process, the mapping of this to a point in the co-domain is calculated. After many repetitions, the correspondence between areas in the domain and the co-domain may be described statistically with increasing confidence.

In this regard, a computer model named SMOKE 2.1 has been specifically written for tunnel fires, as a development of previous works in the field of radiative heat exchanges with non-participating medium [25–27].

5.1.4. Conduction. Assuming convective and radiative heat exchanges (with absorbed and released components) at the wall surfaces to be known, the treatment of the conduction phenomena taking place inside the walls of the tunnel can be carried out by means of the advanced thermo-structural model described in the previous sections.

5.1.5. Complete thermal model. All sub-models described in the previous paragraphs are strongly related to each other.

The fluid dynamics (with the related temperature and velocity fields) depends on wall temperatures and heat generation/sink inside the fluid; the wall temperatures result from the thermal balance among conduction, convection and radiation; the heat generation/sink depends on radiation and chemical reactions; radiation is affected by temperature and composition of the fluid, which in turn are a consequence of fluid dynamics; even combustion, if the chemistry

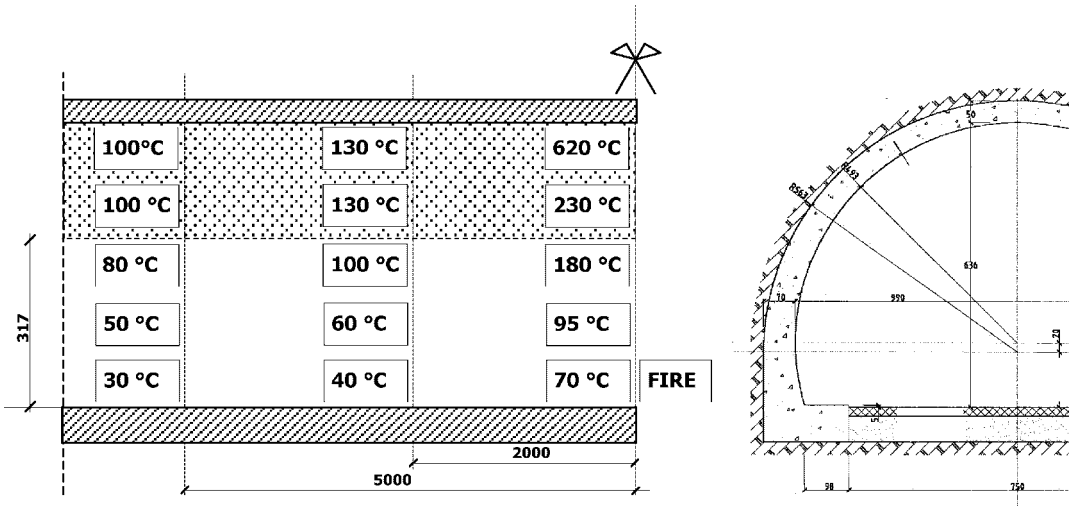

Figure 1. Schematic representation of the longitudinal section of the tunnel, with the position of fire, smoke and maximum temperatures in the instrumented sections at 0, 20 and 50 m from the flames.

of the reaction is correctly accounted for, depends on the fluid dynamics (e.g. as far as soot production is concerned).

Therefore, in order to link together all sub-models an iterative procedure is the most advisable for the moment, considering also that most sub-models are actually independent computer codes.

In practice, after a suitable discretization for fluid and walls has been chosen, the following steps can be taken at each considered time:

1. the energy released by combustion is assumed, according to a given fire scenario;
2. the reaction zone is defined, depending on the location and amount of fuel involved;
3. the heat generation per unit volume is calculated by means of Equation (68);
4. a reasonable distribution of the temperature is assumed;
5. the radiation absorbed by each element is calculated according to Section 5.1.3;
6. the convective heat transfer at the walls is calculated by CFD;
7. the surface temperature are determined as described in Section 5.1.4.

If the temperature field obtained in step 7 is different from that assumed in step 4, the process is repeated with the temperature distribution resulting from steps 6 and 7, until a satisfactory convergence is reached.

5.2. Case study

The simulation procedure described in the previous paragraphs has been applied to a fire scenario for which some experimental measurements were available, see Reference [28], Figure 1. Since the measurements already provided the temperatures of the fluid in several points inside the tunnel, some of the steps discussed in Section 5.1.5 could be skipped.

In details, steps 1–3 could be omitted, whereas for step 4 only the surface temperatures had to be reckoned.

Then, as far as step 5 was concerned, the following assumptions were made. The fluid was divided into two layers, the lower one (up to 3.17 m from the road) made of fresh air at ambient temperature, the upper one (from 3.17 m up to the vault) consisting of smoke with 20% CO_2, 10% H_2O (percentages by volume) and a scattering coefficient (for short wave only) $\rho_{\Delta x}$=0.006, with $\Delta x = 0.1$ m.

Considering the plume of fire at a temperature $T_0 = 1200°C$ and emitting a radiative power $q_r = 2.5$ MW, the absorbed components at the walls (the quantities absorbed by the fluid are of no use in this case) were calculated with a reflectance $\rho = 0.25$ for the vault and $\rho = 0.15$ the road.

Additionally, also the mutual radiation between the walls and smoke was calculated assuming the walls as black bodies. As far as step 6 was concerned, since the fluid temperatures were already known, CFD simulations were not used for the sake of simplicity, and the convective heat transfer was estimated from the correlations given in Reference [29]. Heat transfer coefficient was equal to $27\,W/m^2\,K$ in the zone affected by the plume.

At this point the thermo-structural model was applied and the temperatures and stresses were calculated. It has been assumed that the fire acted with maximum energy for a time span of 20 min maintaining stationary conditions for fire. In the real fire test, the firemen began to extinguish the fire after 5 min. The extra 15 min have been simulated to analyse a further evolution of the hygro-thermo-mechanical behaviour of the concrete vault, assuming that the heat fluxes are the same as during the first 5 min of fire.

It is possible to note the sharp desaturation process interesting the layer of concrete close to the heated surface (Figure 2) and the thermo-diffusion inside the pores of the material.

No visible vault deterioration has been observed during the experimental test. However, the numerical calculations showed that because of the temperatures reached, a considerable thermo-chemical damage is present in the layer of concrete directly exposed to fire, in the three considered locations. This is mainly due to the high temperatures reached, about 600 K after 5 min and 980 K after 20 min (Figure 4), which induce thermo-chemical changes in the microstructure of the material in terms of porosity and permeability. Also, mechanical features of concrete are affected by these processes (i.e. dehydration and cracking) and this leads to a damaging of material. A thermal dilatation of the surface vault layer, while the internal part remained at the initial temperature, caused a considerable mechanical damage of the surface layer of the vault, what contributes to the total concrete damage, Figure 3.

In presence of a mechanical and thermo-chemical damage of the concrete, i.e. when the thermal front deeply enters into the wall causing differential thermal dilatation for a larger depth of material, significant values of pore vapour pressure can produce a separation of superficial layers of concrete, phenomenon known as spalling [17, 20–22, 30]. With the increase of the fire duration, a risk of this phenomenon significantly increases.

6. NUMERICAL SIMULATION OF EXPERIMENTAL MOISTURE FLOW MEASUREMENT

A comparison between experimental test (gamma-ray test) results and the corresponding numerical analysis is presented and discussed to validate the model here proposed, in the case of its application to concrete structures subjected to high temperature.

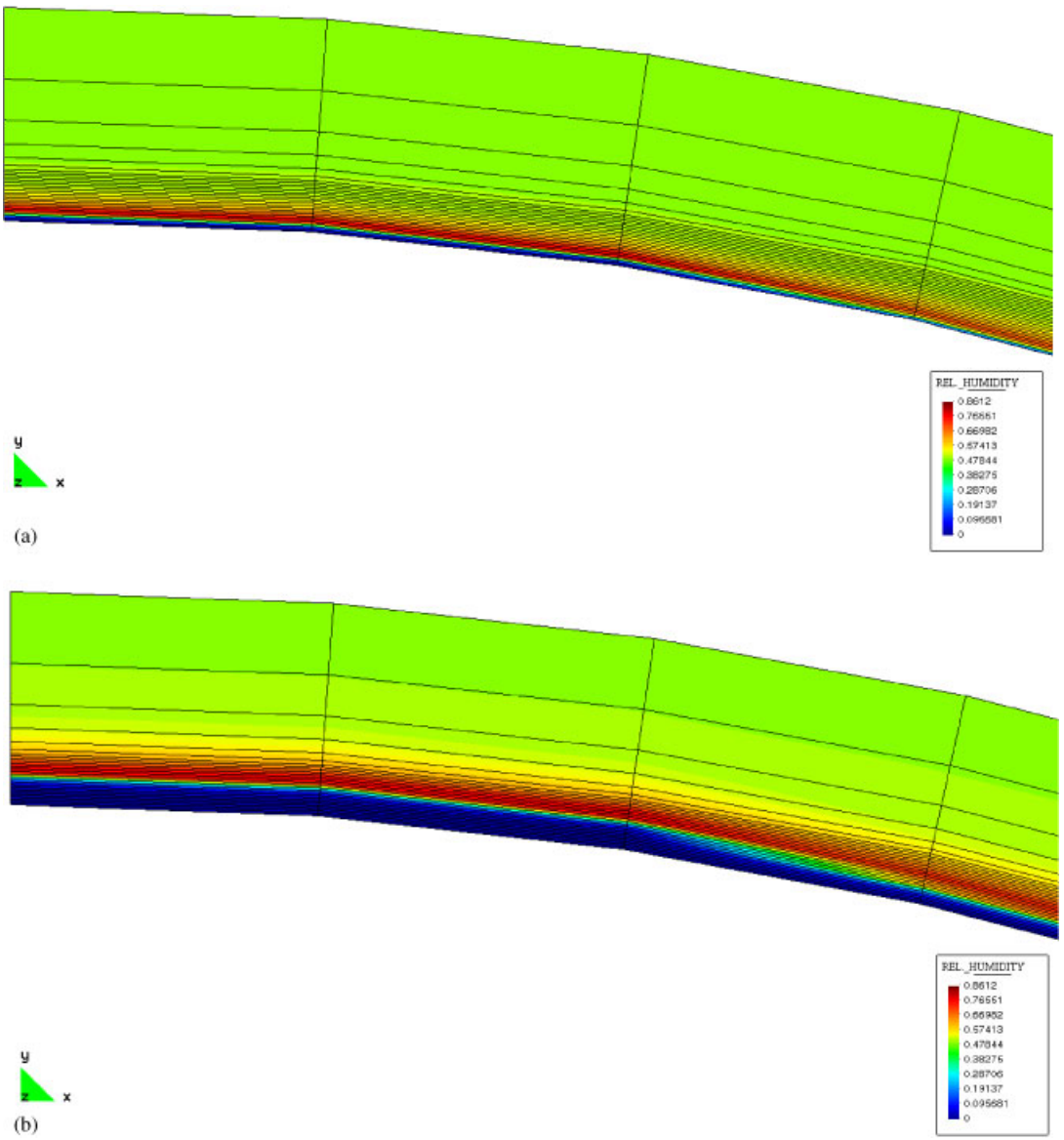

Figure 2. Relative humidity distribution in the top part of the vault of the tunnel after: (a) 5 min; and (b) 20 min.

Gamma-ray spectrometry has been extensively used for determining density moisture content of soils, and is now adapted to various kinds of materials. Interaction between an electromagnetic radiation and matter constitutes the physical basis of this method. Gamma rays emitted by a radioactive material are absorbed by the matter they go through, either partially or totally, depending upon the energy of the photons, the nature and the thickness of the absorber.

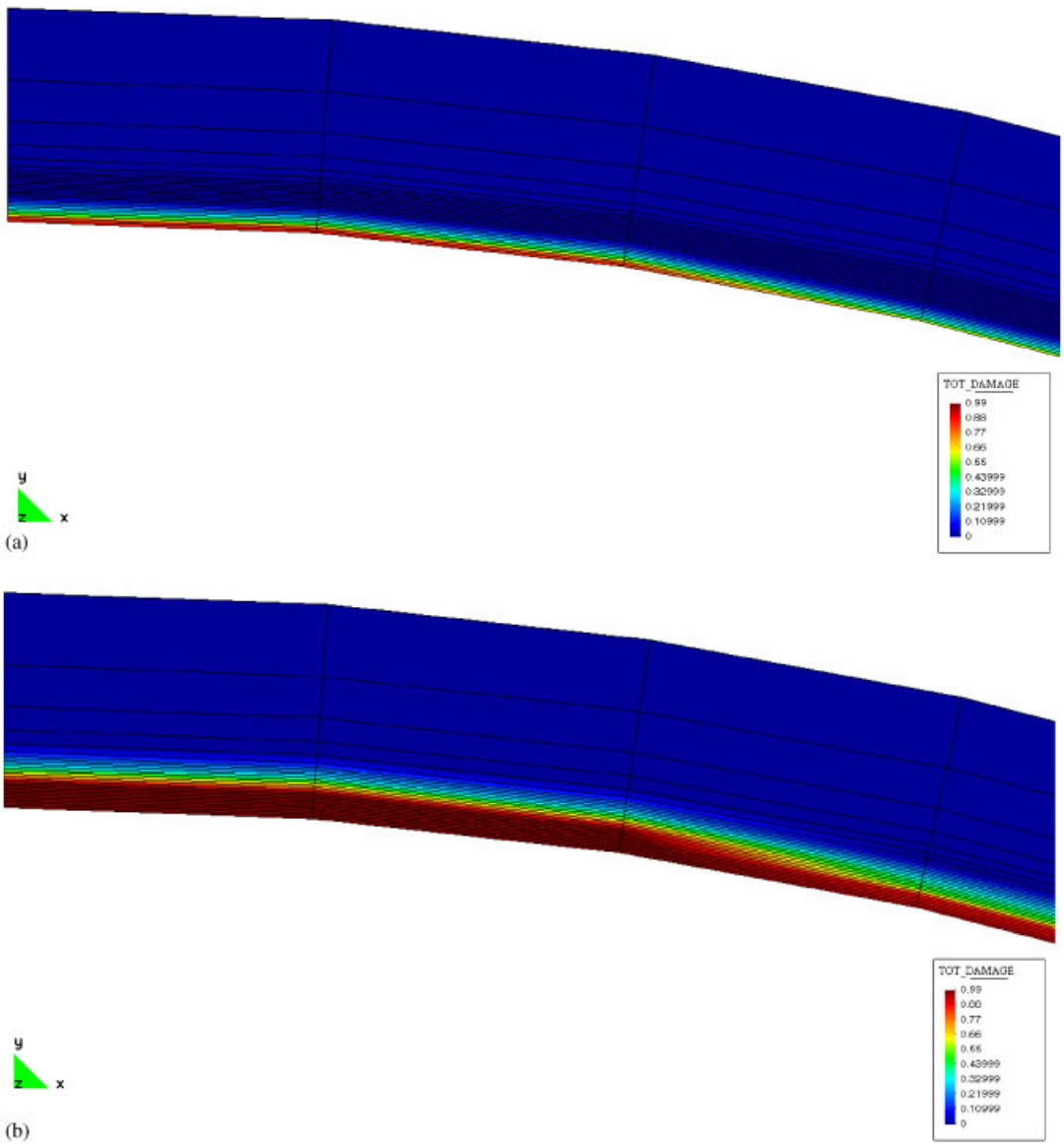

Figure 3. Total damage distribution in the top part of the vault of the tunnel at: (a) 5 min; and (b) 20 min.

This gamma-ray test aims at determining heat transport and moisture content in a piece of concrete heated on one face. It is used in particular to set up the isotherms of desorption and to confirm the validity of the laws employed in the model.

The experimental test was carried out in the framework of BRITE Euram 'Hiteco' research project by Kalifa [31] from the CSTB laboratories in Grenoble.

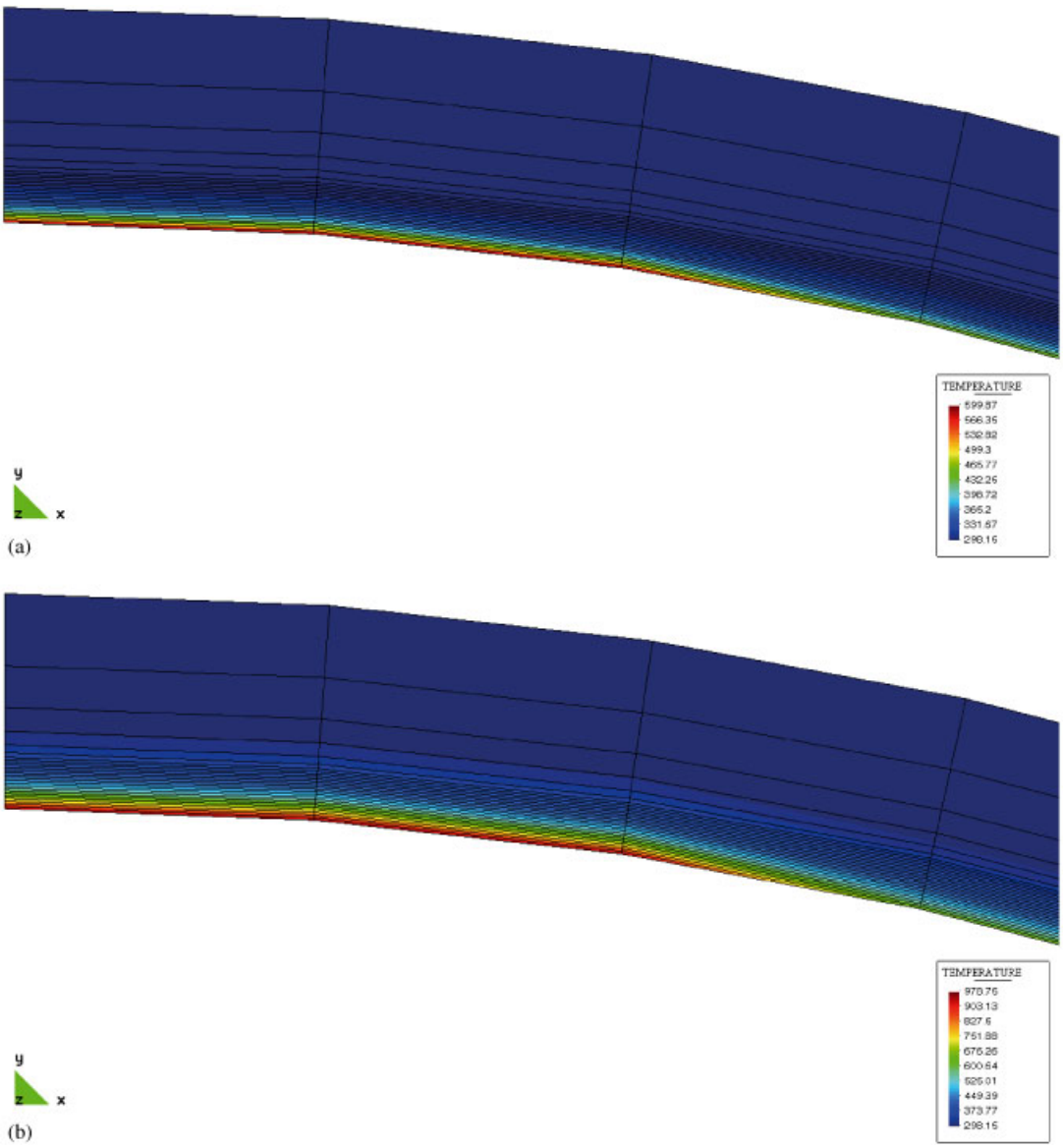

Figure 4. Temperature distribution in the top part of the vault of the tunnel at: (a) 5 min; and (b) 20 min.

The experimental set-up was designed to provide quasi-monodimensional heat and mass transfers in the specimen. Temperature and moisture distribution along the specimen have been measured during heating.

The specimens were cylinders with a length of 100 mm and a diameter of 60 mm for HPC (90 MPa compressive strength). They were provided with seven thermocouples (fibre glass

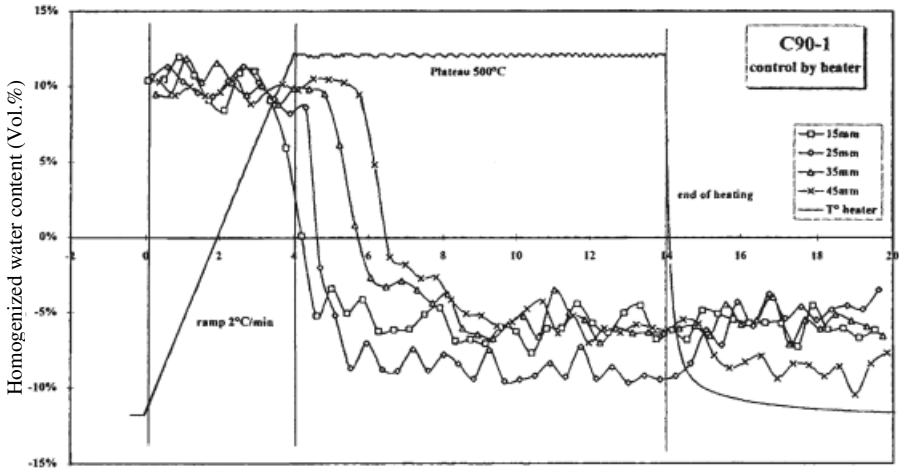

(a)

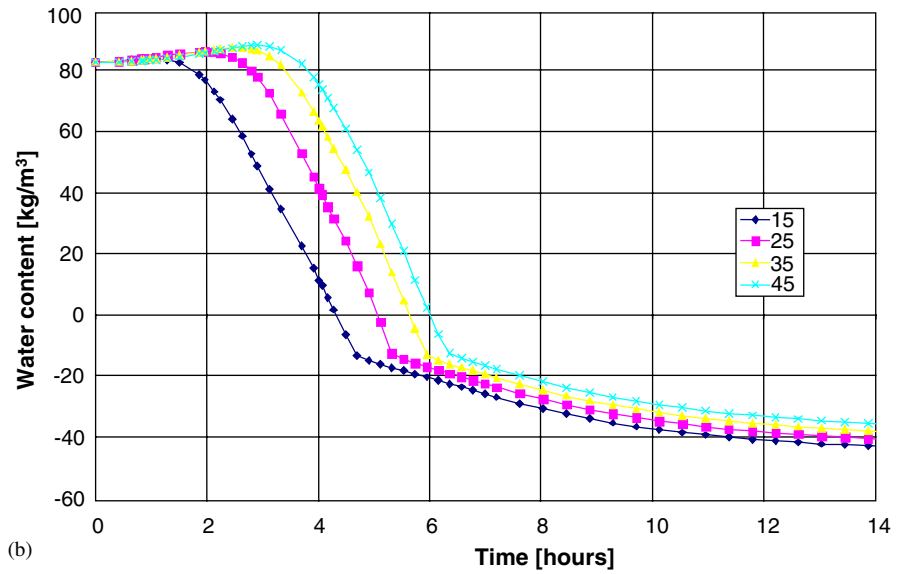

(b)

Figure 5. (a) Water content in different points recorded in gamma-ray test [31]; and (b) corresponding water content from numerical simulation.

jacket) installed at casting at 2, 10, 20, 30, 40, 50 and 75 mm from the heated face. The specimen was heated on one end with a flat radiant (51 kW/m^2) heater located at about 1 cm from the specimen and fixed on the carriage.

The gamma-ray generator and detector/analyser were placed on an axis perpendicular to the displacement axis.

For more detailed information about the experimental set-up the reader is referred to Reference [31].

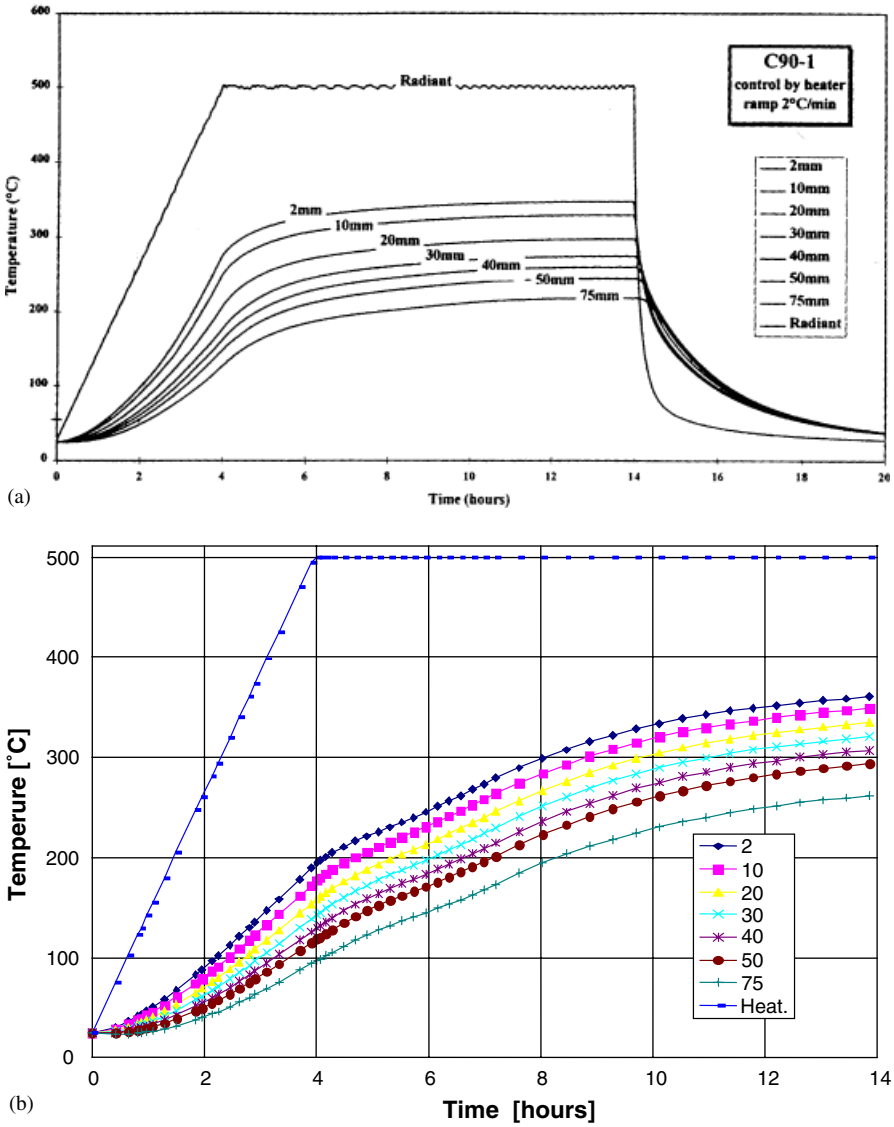

Figure 6. (a) Temperatures in different points recorded in gamma-ray test [31]; and (b) corresponding temperatures from numerical simulation.

The reference measurement related to each position was made before heating and water loss refers to the initial value, Figure 5.

The problems related to measurements of water content through gamma-ray test regard mainly the correct interpretation of the results, in particular the meaning of negative values of water content which appear from a certain moment on, Figure 5. In fact, because of dehydration the quantity of water in cement gel, which is part of solid phase, changes and more exactly

decreases. Thus, there is an additional water loss whose contribution yields negative values of water content (Figure 5) because they are referred to free water content initial values.

The results of the experimental test and the corresponding numerical results are reported in Figures 5 and 6, in the form of moisture content and thermal field, respectively. The results of numerical simulation show a good agreement with experimental ones. In particular for the moisture content the time corresponding to zero water content, i.e. a quantity of water equal to initial free water content has been released, is substantially the same. This means that the kinetic of the process has been well simulated by the code.

The values on the vertical axis are not directly comparable because of the different reference state. The absolute values of moisture content in the numerical results are expressed in kg/m^3, Figure 5(b). As clearly visible from Figure 5, taking into account that at the beginning saturation degree is 0.8 and porosity is 0.1 the initial water content corresponds to 8–9% of the experimental results. As for thermal fields, temperatures obtained from calculation are slightly lower than real values. This could be due to the uncertainty of boundary conditions.

7. CONCLUSIONS

In this paper, a thermodynamically consistent model for heat and mass transfer in deforming porous media, including phase changes, has been developed. Hybrid mixture theory has been used for this purpose and interface properties have been included. From this theoretical model, a simplified numerical model has been extracted and subsequently validated by means of a comparison between experimental results concerning gamma-ray test and the corresponding numerical analysis. This model is used for simulating the behaviour of heated concrete in tunnel fires. Significant phenomena such as spalling and thermal diffusion have been evidenced. This application shows, together with other not reported here, that the model is extremely versatile.

ACKNOWLEDGEMENTS

I wish to thank Profs. P. Brunello and D. Gawin and Dr F. Pesavento for their valuable contribution in preparing the paper. This work has been partly financed by the EU research fund MÆCENAS ‘Modelling of Ageing in Concrete Nuclear Power Plant Structures’.

REFERENCES

1. Hassanizadeh M, Gray WG. General conservation equations for multiphase systems: 1 averaging procedure. *Advances in Water Resources* 1979; **2**:131–144.
2. Hassanizadeh M, Gray WG. General conservation equations for multiphase systems: 2 mass, momenta, energy and entropy equations. *Advances in Water Resources* 1979; **2**:191–203.
3. Hassanizadeh M, Gray WG. General conservation equations for multiphase systems: 3 constitutive theory for porous media flow. *Advances in Water Resources* 1980; **3**:25–40.
4. Hassanizadeh M, Gray WG. Mechanics and thermodynamics of multiphase flow in porous media including interphase transport. *Advances in Water Resources* 1990; **13**:169–186.
5. Schrefler BA. Thermodynamics of saturated-unsaturated porous materials and quantitative solutions: the isothermal case. *Proceedings of the 2nd European Conference on Computational Mechanics*, Cracow, Poland, 2001.
6. Coleman BD, Noll W. The thermodynamics of elastic materials with heat conduction and viscosity. *Archives for Rational Mechanics and Analysis* 1963; **13**:168–178.

7. Lewis RW, Schrefler BA. *The Finite Element Method in the Deformation and Consolidation of Porous Media*. Wiley: Chichester, 1987.
8. Schrefler BA. Mechanics and thermodynamics of saturated-unsaturated porous materials and quantitative solutions, *Applied Mechanics Reviews* 2002; **55**:357–388.
9. Gray WG, Hassanizadeh M. Unsaturated flow theory including interfacial phenomena. *Advances in Water Resources* 1991; **27**:1855–1863.
10. Gray WG, Hassanizadeh M. Paradoxes and realities in unsaturated flow theory. *Advances in Water Resources* 1991; **27**:1847–1854.
11. Bennethum LS, Cushman JH. Multiscale, hybrid mixture theory for swelling systems-I: balance laws. *International Journal of Engineering Science* 1996; **34**(2):125–145.
12. Bennethum LS, Cushman JH. Multiscale, hybrid mixture theory for swelling systems-II: constitutive theory. *International Journal of Engineering Science* 1996; **34**(2):147–169.
13. Bennethum LS, Murad MA, Cushman JH. Macroscale thermodynamics and the chemical potential for swelling porous media. *Transport in Porous Media* 2000; **39**(2):187–225.
14. Bennethum LS. 2001, private communication.
15. Hassanizzadeh M. Derivation of basic equations of mass transport in porous media, part 2 generalized Darcy's and Fick's law. *Advances in Water Resources* 1986; **9**:207–222.
16. Baggio P, Bonacina C, Schrefler BA. Some considerations on modelling heat and mass transfer in porous media. *Transport in Porous Media* 1997; **28**:233–281.
17. Gawin D, Pesavento F, Schrefler BA. Modelling of hygro-thermal behaviour and damage of concrete at temperature above the critical point of water. *International Journal for Numerical and Analytical Methods in Geomechanics* 2002; **26**:537–562.
18. Ulm FJ, Coussy O, Bazant ZP. The 'Chunnel' fire. I: chemoplastic softening in rapidly heated concrete. *Journal of Engineering Mechanics* (ASME) 1999; **125**(3):272–282.
19. Ulm FJ, Acker P, Lévy M. The 'Chunnel' fire. II: analysis of concrete damage. *Journal of Engineering Mechanics Transactions* (ASME) 1999; **125**(3):283–289.
20. Gawin D, Majorana CE, Schrefler BA. Numerical analysis of hygro-thermic behaviour and damage of concrete at high temperature. *Mechanics of Cohesive-Frictional Materials* 1999; **4**:37–74.
21. Gawin D, Pesavento F, Schrefler BA. Simulation of damage—permeability coupling in hygro-thermo-mechanical analysis of concrete at high temperature. *Communications in Numerical Methods in Engineering* 2002; **18**:113–119.
22. Pesavento F. Non-linear modelling of concrete as multiphase porous material in high temperature conditions. *Ph.D. Thesis*, University of Padova, Padova, 2000.
23. Xue H, Ho JC, Cheng YM. Comparison of different combustion models in enclosure fire simulation. *Fire Safety Journal* 2001; **36**(1):37–54.
24. Rubenstein RY. *Simulation and the Monte Carlo Method*. Wiley: New York, 1981.
25. Brunello P. Solar pressure evaluation on large reflectors for space applications. *Communications in Applied Numerical Methods* 1993; **9**(10):787–795.
26. Brunello P, Gnesotto F, Majorana CE, Schrefler BA. Thermal analysis of a graphite first wall for fusion experiment RFX. *Communications in Applied Numerical Methods* 1988; **4**:647–656.
27. Brunello P, Zecchin R. A Monte-Carlo Approach for the design of high temperature heating panels. *Proceedings of the International Symposium Energy Conservation in the Built Environment* 1993; CIB Publication 152, IRB-Verlag: Stuttgart, Germany, 1993.
28. Ministry of Internal Affairs. *Fire Test in Highway Tunnel*, Corpo Nazionale dei Vigili del Fuoco, Roma, Italy, 2000 (in Italian).
29. Karlsson B, Quintiere JG. *Enclosure Fire Dynamics*. CRC Press: Boca Raton, FL, 2000.
30. Schrefler BA, Brunello P, Gawin D, Majorana CE, Pesavento F. Concrete at high temperature with application to tunnel fire. *Computational Mechanics* 2002; **29**(1):43–51.
31. Brite Euram III BRPR-CT95-0065 HITECO. Understanding and industrial application of high performance concrete in high temperature environment. *Final Report*, 1999.

